International Journal of GEOMATE, Dec., 2018 Vol.15, Issue 52, pp.222-229
Geotec., Const. Mat. & Env., DOI: https://doi.org/10.21660/2018.52.96300
ISSN: 2186-2982 (Print), 2186-2990 (Online), Japan

FATIGUE AND AGGREGATE FRETTING RESISTANCE OF SURFACE-TEMPERATURE REDUCING PAVEMENT

* Hiroshi Higashiyama[1], Hiromu Inoue[1], and Manote Sappakittipakorn[2]

[1] Faculty of Science and Engineering, Kindai University, Japan
[2] Faculty of Engineering, King Mongkut's University of Technology North Bangkok, Thailand

*Corresponding Author, Received: 11 Jul. 2018, Revised: 2 Aug. 2018, Accepted: 03 Oct. 2018

ABSTRACT: In the field of road engineering, cool pavements are used to decrease the surface temperature and improve the road environment. A surface-temperature reducing pavement was previously developed using a cement-based grouting material containing cement, ceramic waste powder, and natural zeolite. From the temperature measurements, it was revealed that the surface temperature was lower by 15-20°C than the porous asphalt pavement at 60°C. The pavements can undergo rutting under passing traffic loads and aggregate fretting in the hot summer season, lowering serviceability and traffic safety. Fatigue tests under a fixed-point load were conducted to evaluate the fatigue resistance of the surface-temperature reducing pavement at 40°C imitating the hot summer season. In this study, fatigue tests under a fixed-point load at 30°C imitating the spring or autumn season were carried out to evaluate the fatigue resistance against the rutting. Furthermore, the aggregate fretting tests were carried out to evaluate the aggregate fretting resistance at temperatures of 50°C and 30°C. The test results showed that the surface-temperature reducing pavement has higher fatigue and aggregate fretting resistance than the porous asphalt pavement.

Keywords: Cool pavement, Fixed-point fatigue load, Fatigue resistance, Aggregate fretting resistance

1. INTRODUCTION

Asphalt and concrete pavements cover a high percentage of urban areas and largely affect the development of the heat island phenomenon. One of the countermeasures against the heat island phenomenon is cool pavements increasingly constructed in urban areas to decrease the surface temperature and improve the road environment [1, 2]. In our previous studies [3, 4], a surface-temperature reducing pavement was developed by using ultra-rapid hardening cement, ceramic waste powder, and natural zeolite. The outdoor measurements showed that the pavement reduced the surface temperature by 15-20°C in comparison with the porous asphalt pavement at 60°C in the hot summer.

Unfortunately, permanent deformation such as rutting and aggregate fretting of porous asphalt pavements seriously affects the driving safety and the serviceability of traffic vehicles. The permanent deformation results from strain accumulating in the asphalt mixture under passing traffic loads and higher shear stress acting over time [5]. A higher resistance against such permanent deformation increases the fatigue life of asphalt pavements [6]. The cool pavements, as well as semi-flexible asphalt pavements, are helpful to reduce such rutting [7].

The aim of this study is to evaluate the fatigue resistance to the rutting and the aggregate fretting resistance of the surface-temperature reducing pavement developed previously. In this paper, fatigue tests were carried out under a fixed-point load with different loading levels in water at 30°C and aggregate fretting tests at 50°C and 30°C for the surface-temperature reducing pavement and the porous asphalt pavement. In the fixed-point fatigue tests, the fatigue life up to a certain sinking displacement at the loading point, which was regarded as the rutting depth, was compared with that of the porous asphalt pavement as in the previous fatigue test [8]. Furthermore, in the aggregate fretting tests using a wheel trucking machine, the aggregate fretting resistance by the torsion assumed at the intersection was evaluated.

2. FIXED-POINT FATIGUE TESTS

2.1 Cement-Based Grouting Material

The cement-based grouting material was prepared using ultra-rapid hardening cement (UHC), ceramic waste powder (CWP), and natural zeolite (NZ). The ceramic waste powder, which was collected in the recycling process of ceramic waste porcelain insulators, was provided from the Kanden L&A Co., Ltd, Japan. The natural zeolite with a particle size of fewer than 200 μm was mined in Izumo, Shimane, Japan. The chemical and physical properties are shown in Table 1. The mixing ratio of UHC, CWP, and NZ was

0.5:0.35:0.15 by weight. The water-to-cement ratio (w/c) was kept constant at 1.3 by weight. To increase the workability of the cement-based grouting material and the labor time during infiltration into voids in the porous asphalt pavement, an air entraining and high-range water reducing agent provided from BASF Japan Ltd., Japan and a setting retarder were added by 3% and 0.4% of the UHC by weight, respectively [8].

The compressive strength development of the cement-based grouting material is shown in Fig.1 with the results obtained in the previous study [8]. Three cylindrical specimens with a diameter of 50 mm and a height of 100 mm were used for each curing age. The curing condition was in the arbitrary room temperature with no control, which was the same curing condition for the surface-temperature reducing pavements used in the fatigue tests. At 28 days, the compressive strength was 14.7 N/mm^2 in this study. The fatigue test was started after 28 days of curing because the compressive strength became stable. The strength development agreed with the results in the previous study [8].

2.2 Specimens

The asphalt mixture used in this study was the same as in the previous study [8] and designed with a void ratio of 23% using the straight asphalt with a 60/80 penetration and an addition of 3.5% by weight. The specimen had a square size of 650×650 mm and a total thickness of 100 mm. The porous asphalt pavement with a thickness of 50 mm was paved on a hard rubber plate with a thickness of 50 mm as shown in Fig.2. The hard rubber plate had a hardness of 65±5, Young's modulus of 3.42 N/mm^2, and a shear elastic modulus of 1.14 N/mm^2. Totally, ten porous asphalt pavements were compacted using a roller compactor at a temperature of about 150°C. After the temperature of the porous asphalt pavement decreased and the surface temperature reached 35°C, the cement-based grouting material was poured and vibrated on the surface for five specimens. Finally, the surface was treated with a rubber lake to keep it smooth as shown in Fig.3. The porous asphalt pavements with and without the cement-based grouting material were prepared for each of five specimens. In this paper, the specimen of the porous asphalt pavement is called PoAs and the specimen with the cement-based grouting material is called JGZ.

2.3 Test Method

The specimen placed in an aluminum mold was fixed in a water tank and fully soaked in water at 30°C controlled by an electric heater. When the atmospheric temperature is 20°C, which imitates the spring or autumn season, the average

Table 1 Chemical and physical properties

Properties	CWP	NZ
Chemical compositions (wt.%)		
SiO_2	70.90	70.15
Al_2O_3	21.10	12.28
Fe_2O_3	0.81	1.16
Cao	0.76	1.98
MgO	0.24	0.53
Na_2O	1.47	1.93
K_2O	3.57	2.38
TiO_2	0.33	0.17
MnO		0.06
Loss on ignition		9.25
Specific gravity	2.43	2.30
Specific surface area (cm^2/g)	1810	6770

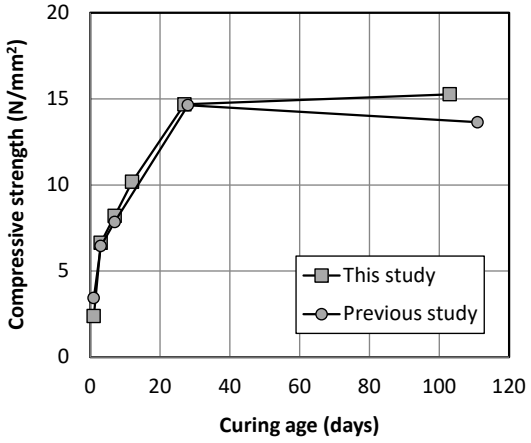

Fig.1 Compressive strength development

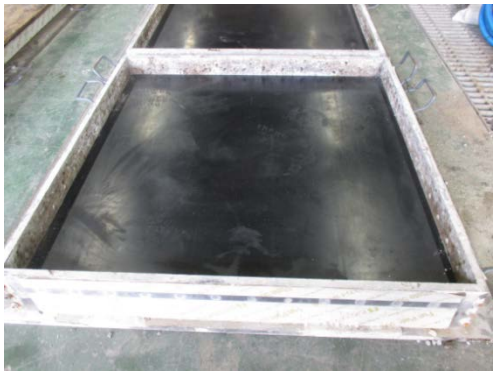

Fig.2 A hard rubber plate with a thickness of 50mm placed at the bottom

temperature of the conventional asphalt pavement along the depth is about 30°C [9]. In this test, the water temperature was thus determined to be 30°C. In the previous study [8], the water temperature was 40°C imitating the summer season of the

atmospheric temperature at 30°C. In this paper, the fatigue resistances at both temperatures were compared. The surface of the water tank was covered by styrene form plates except the loading plate area to prevent evaporation and temperature reduction of the water as shown in Fig.4. After the specimen was kept in the 30°C water for 24 h, the fatigue test was started under the fixed-point load. The water level in the tank was kept constant during the fatigue test. As shown in Fig.5, the loading steel plate of 150×60 mm, which was the same as in the previous study [8], was similar to the contact area (500×200 mm) of the rear tire has a design wheel load specified by Japanese Specifications for Roadway Bridges [10]. Then, the tire contact pressure was 1.0 N/mm^2. The maximum load applied was varied from the contact pressure of 1.0 N/mm^2 considering the sinking behavior of specimens during the fatigue test as shown in Table 2. Also, the minimum load applied was kept at 0.5 kN. As the loading condition, a sine wave with a frequency of 3 Hz was applied in load control.

The sinking displacement at the loading point was automatically measured at intervals by four linear variable-differential transducers (LVDTs) with a 25 mm capacity attached to the corners of the loading plate. The acquisition speed of the LVDTs was 1000 Hz so as to measure the maximum and minimum displacements with adequate accuracy under the cyclic loading. The interval of the data acquisition was 5 min.

As in the previous study [8], the number of loading cycles at the fracture of each specimen was defined as the sinking displacement at both 15 mm and 20 mm. The sinking displacement of 15 mm or 20 mm was usually adopted according to the rutting maintenance level, water splash by vehicles, and hydroplaning phenomenon in the standard maintenance strategies on highway pavements [11, 12]. In this study, the specimen did not reach 20 mm in the fatigue tests up to 3 million loading cycles, then the loading was stopped.

2.4 Results and Discussion

2.4.1 Sinking displacement

The relationships between the sinking displacement at the loading point and the number of loading cycles for some specimens are shown in Fig.6. From Fig.6(a) for the PoAs specimen at the contact pressure of 1.0 N/mm^2, the displacement initially increased due to densification of the asphalt mixture. After that, the behavior rapidly changed to stable deformation following a constant increase rate of the sinking displacement with a de-bonding of asphalt between aggregates and a lateral flow of the asphalt mixture. The same phenomenon was observed in the PoAs specimens at 40°C in the previous study [8]. All of the PoAs specimens reached over the targeted displacement of 20mm.

From Fig.6(b), the JGZ30-2 specimen at the contact pressure of 2.2 N/mm^2 including the JGZ30-1 specimen at the contact pressure of 2.4 N/mm^2 showed almost the same behavior as the PoAs specimen shown in Fig.6(a). However, from a certain number of loading cycles, the increase rate of the displacement gradually accelerated. As the failure process of the JGZ specimens, at the first stage, some cracks occurred in the cement-based grouting material. After that, de-bonding of the asphalt or the cement-based grouting material

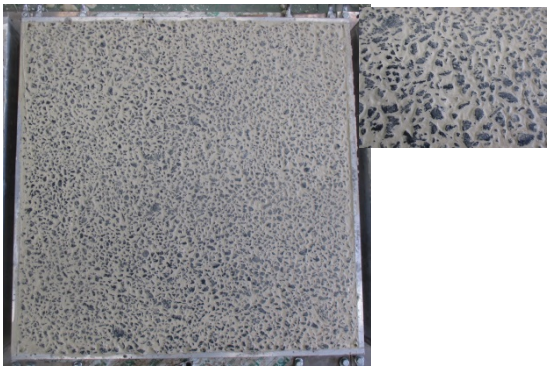

Fig.3 Cement-based grouting material poured into voids of the porous asphalt specimen after surface treatment

Fig.4 Fatigue test setup

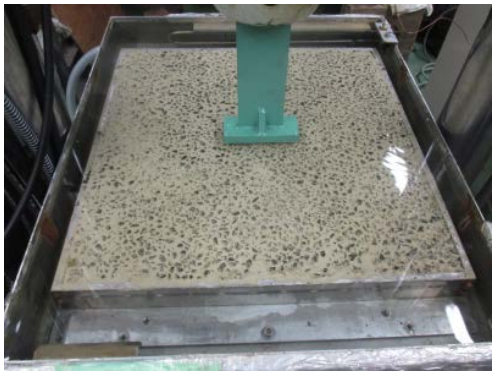

Fig.5 Loading condition

Table 2 Contact pressure applied to each specimen

PoAs	Contact pressure (N/mm^2)	JGZ	Contact pressure (N/mm^2)
PoAs30-1	1.00	JGZ30-1	2.4
PoAs30-2	0.80	JGZ30-2	2.2
PoAs30-3	0.60	JGZ30-3	2.0
PoAs30-4	0.50	JGZ30-4	1.2
PoAs30-5	0.40	JGZ30-5	1.0

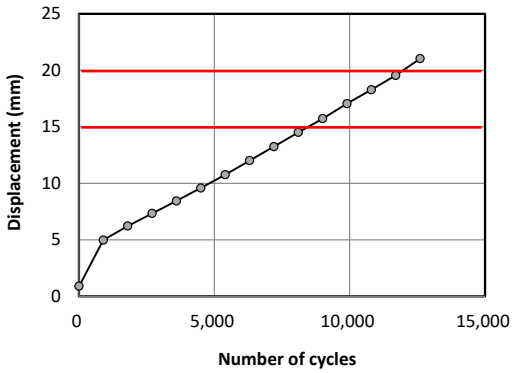

(a) PoAs30-1 (Contact pressure 1.0 N/mm^2)

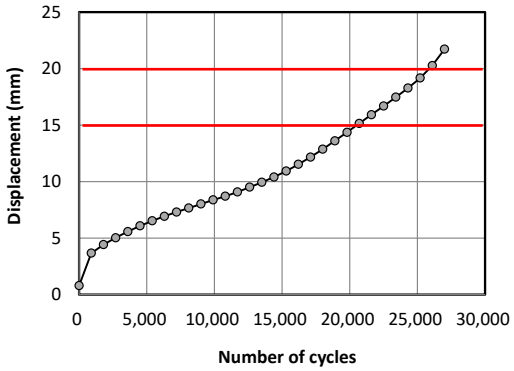

(b) JGZ30-2 (Contact pressure 2.2 N/mm^2)

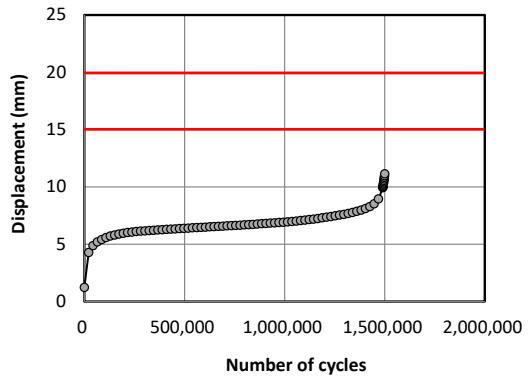

(c) JGZ30-3 (Contact pressure 2.0 N/mm^2)

Fig.6 Sinking displacement at the loading position and the number of loading cycles

between aggregates occurred with a lateral flow of the asphalt mixture. The displacement of the JGZ30-3 specimen at the contact pressure of 2.0 N/mm^2 rapidly increased at about 1.5 million loading cycles as shown in Fig.6(c). After that, the operating capacity of the test machine, however, exceeded due to the rapid increase of displacement. From this behavior, it was determined that the failure of the specimen occurred at around 1.5 million loading cycles. The JGZ30-4 and JGZ30-5 specimens showed lower displacement than the other specimens and behaved to increase stable up to 3 million loading cycles. Finally, they did not reach the sinking displacement of 15 mm.

2.4.2 Fatigue life

All of the PoAs specimens and the JGZ30-1 and JGZ30-2 specimens reached over the targeted displacement of 20 mm. In contrast, the JGZ30-3 specimen did not reach over 15 mm as mentioned above. Hence, the number of loading cycles at each 15 mm and 20 mm in the JGZ30-3 specimen was estimated by the linear approximation method from the rapidly increasing trend. Unfortunately, for the JGZ30-4 and the JGZ30-5, each displacement was too low to estimate the number of loading cycles at the targeted displacements of 15 mm and 20 mm. Therefore, these specimens were excluded from the comparison for the fatigue life. The number of loading cycles at the displacements of 15 mm and 20 mm are listed in Table 3 for the PoAs specimens and Table 4 for the JGZ specimens including the test results at 40°C in the previous study [8].

From the fatigue life given in Tables 3 and 4, the relationships between the contact pressure and the number of loading cycles are plotted in the S-N diagram at each targeted displacement as shown in Fig.7. It can be seen that the data points obtained in this study are also linearly plotted in each S-N diagram as in the previous study tested at 40°C [8]. From these results, the fatigue strength was sensitive with the temperature. Furthermore, at

Table 3 Fatigue life of PoAs specimens at each sinking displacement

Test condition (°C)	Specimen	Contact pressure (N/mm^2)	Fatigue life (cycles)	
			15 mm	20 mm
30°C	PoAs30-1	1.00	8,467	11,975
	PoAs30-2	0.80	12,178	17,062
	PoAs30-3	0.60	45,516	57,476
	PoAs30-4	0.50	321,563	356,601
	PoAs30-5	0.40	183,925	229,373
40°C	PoAs40-1	1.00	1,566	1,993
	PoAs40-2	0.90	1,857	2,462
	PoAs40-3	0.80	1,647	2,257

	PoAs40-4	0.50	8,729	11,456
	PoAs40-5	0.40	11,030	14,944

Table 4 Fatigue life of JGZ specimens at each sinking displacement

Test condition (°C)	Specimen	Contact pressure (N/mm²)	Fatigue life (cycles) 15 mm	20 mm
30°C	JGZ30-1	2.40	8,254	10,538
	JGZ30-2	2.20	20,532	25,880
	JGZ30-3	2.00	1,515,190*	1,527,350*
40°C	JGZ40-1	1.10	2,785	3,913
	JGZ40-2	1.00	67,778	84,076
	JGZ40-3	0.95	1,663,200	7,120,796*

*The number of loading cycles estimated by linear approximation.

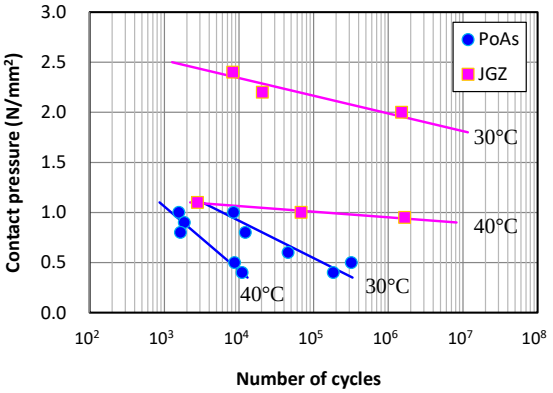

(a) Fatigue life at the sinking displacement of 15 mm

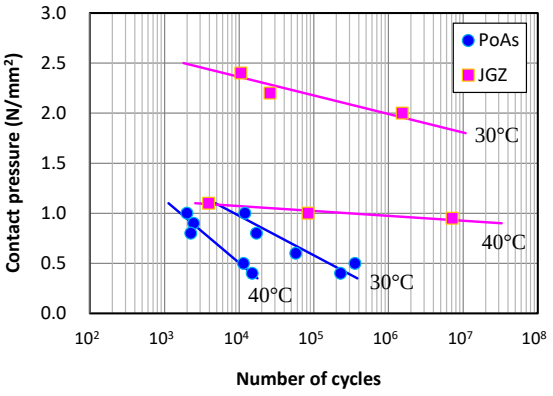

(b) Fatigue life at the sinking displacement of 20 mm

Fig.7 Contact pressure and fatigue life

each temperature, the JGZ pavement had a greatly higher fatigue life than the porous asphalt pavement. The difference in the fatigue life of the JGZ pavement between the two temperatures was very large beyond comparison. Each S-N curve can be summarized in Table 5.

Table 5 S-N curves for each pavement

Pavement	Test condition (°C)	Rutting depth (mm)	S-N curve
JGZ	30	15	logN = -5.660σ+17.254
		20	logN = -5.403σ+16.760
	40	15	logN = -17.844σ+22.974
		20	logN = -20.532σ+25.997
PoAs	30	15	logN = -2.681σ+6.458
		20	logN = -2.537σ+6.471
	40	15	logN = -1.569σ+4.662
		20	logN = -1.590σ+4.807

3. AGGREGATE FRETTING TESTS

3.1 Specimens

The asphalt mixture used in this test was the same as the specimen in the fix-point fatigue test mentioned above. Namely, it was designed with a void ratio of 23% using the straight asphalt with a 60/80 penetration and an addition of 3.5% by weight. The specimen had a square size of 300×300 mm and a thickness of 50 mm. Totally, welve porous asphalt pavements were compacted using a compactor at a temperature of about 150°C. The cement-based grouting material was poured into the voids and vibrated on the surface for six specimens. Finally, the surface was treated with a rubber lake to keep it smooth. The porous asphalt pavements with and without the cement-based grouting material were prepared for each of the six specimens. The compressive strength after 28 days of curing was 15.9 N/mm^2. It almost agreed on the results shown in Fig.1. The aggregate fretting test for the JGZ specimen started after 28 days of curing because the compressive strength became stable.

3.2 Test Method

In the aggregate fretting test, a wheel trucking machine shown in Fig.8 was used. This is a standard test method for drainage asphalt pavements specified by the Japan Road Association [13]. The specimen placed in an aluminum mold was fixed on a rotating table of the wheel trucking machine. Using a handcart tire with a diameter of 200 mm and a width of 65 mm, a constant load of 490 N (contact pressure of 0.43 N/mm^2) was applied onto the specimen. The air pressure and the rotating radius of the handcart tire were 200±10 kPa and 75 mm. The rotating speed of the wheel trucking machine was constant at 10.5 rpm and the testing period for each specimen was within 120 min as specified in the Japan Road

As [illegible] he

Fig.8 Aggregate fretting test

atmospheric temperature condition of 50°C and 30°C. After keeping each specimen at the preset temperature for over 5 h in a dry condition, the test was started. The weight of specimen in which scattered aggregates and other dust were completely removed was measured at an interval of 30 min until 120 min, and the weight ratio was calculated from the weight before testing and after each interval as the aggregate fretting ratio.

3.3 Results and Discussion

3.3.1 Surface condition after testing

The surface conditions of the PoAs specimens after the aggregate fretting test at both 30°C and 50°C are shown in Fig.9. The aggregate fretting was observed at an early stage within 30 min loading at 30°C and 50°C. At 50°C, the asphalt mixture under the wheel was completely scattered before the testing time of 120 min as shown in Fig.9(b). In contrast, as shown in Fig.10, the surface conditions observed in the JGZ specimens after the aggregate fretting test, i.e. after 120 min loading, showed no aggregate fretting and showed only slight abrasion on the surface at both 30°C and 50°C.

3.3.2 Aggregate fretting ratio

The relationship between the aggregate fretting ratio and the testing time at 30°C and 50°C is shown for PoAs specimens in Fig.11 and for JGZ specimens in Fig.12. The dotted lines indicate test data and the solid line indicates the average of the data. In the tests for the PoAs specimens, the different surface condition, i.e. the lower aggregate fretting, in one specimen was observed at both 30°C and 50°C. It might be the influence of compaction and aggregate distribution. Therefore, the result of each specimen was excluded. In the reference [13], the threshold for the aggregate fretting ratio was 20% or less for the drainage asphalt pavement. In this study, the test results were evaluated using this threshold value.

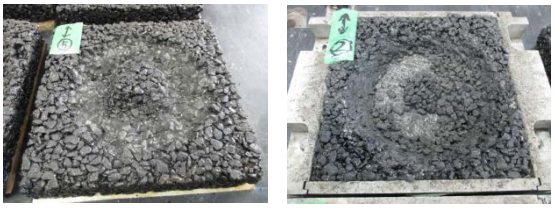

(a) At 30°C (b) At 50°C

Fig.9 Surface condition of PoAs specimen after testing

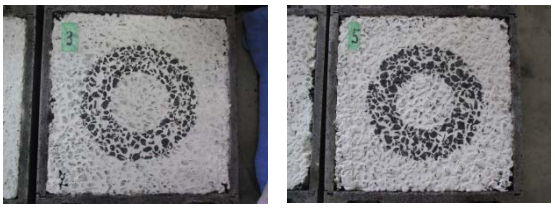

(a) At 30°C (b) At 50°C

Fig.10 Surface condition of JGZ specimen after testing

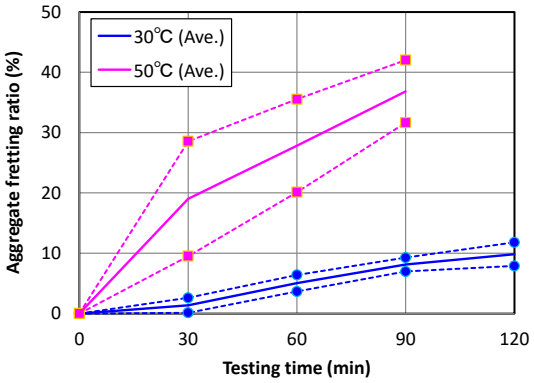

Fig.11 Aggregate fretting ratio and testing time of PoAs specimens

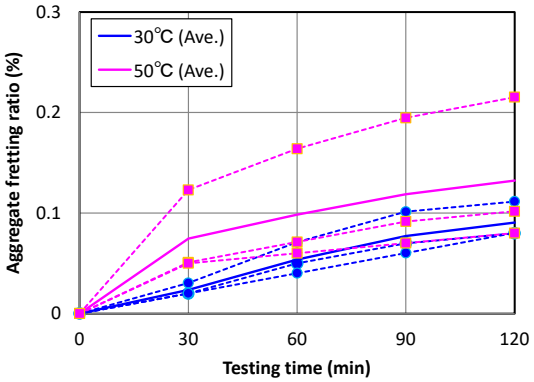

Fig.12 Aggregate fretting ratio and testing time of JGZ specimens

As shown in Fig.11, the average aggregate fretting ratio of the PoAs specimens at 30°C reached 10% in 120 min. At 50°C, the aggregate fretting ratio rapidly increased and the average value exceeded the threshold value of 20% after 30 min. The PoAs specimens had lower resistance against the aggregate fretting because the straight asphalt with a 60/80 penetration was used in this study.

On the other hand, the aggregate fretting ratios of JGZ specimens were very small at both 30°C and 50°C. It can be also seen from Fig.10 that the surface was slightly shaved off. The test results demonstrated that the JGZ pavement had higher resistance against the aggregate fretting.

4. CONCLUSIONS

In this study, the fatigue tests under the fixed-point load and the aggregate fretting tests were carried out to evaluate the resistance of the surface-temperature reducing pavement. The main conclusions are as follows:

(1) In the PoAs pavements, the displacement at the loading point rapidly increased up to the targeted displacement depending on the contact pressures. Under the contact pressure lower than 0.6 N/mm^2, the sinking displacement increased at a constant rate. After that, the increase rate of the displacement gradually accelerated at a certain number of loading cycles.

(2) Under the contact pressure lower than 2.0 N/mm^2, the JGZ pavements did not reach the targeted displacement. The test results obtained in the present and previous studies demonstrated that the JGZ pavement had significantly higher fatigue resistance at both 30°C and 40°C than the PoAs pavement. This can be concluded that the JGZ pavement considerably reduces the rutting over time.

(3) In the aggregate fretting tests, the resistance of the PoAs pavement decreased rapidly. In contrast, only slight abrasion in the JGZ pavement was observed on the surface at both 30°C and 50°C. The test results demonstrated that the JGZ pavement also had higher resistance against the aggregate fretting than the PoAs pavements.

5. ACKNOWLEDGMENTS

The first author wishes to acknowledge the financial support of JSPS KAKENHI (Grant Number JP 16K06451), Japan. The authors are also grateful to Kanden L&A Co., Ltd for providing the ceramic waste powder and BASF Japan Ltd. for providing the chemical admixture.

6. REFERENCES

[1] Santamouris M., Using cool pavements as a mitigation strategy to fight urban heat Island-a review of the actual developments, Renewable, and Sustainable Energy Reviews, Vol. 26, 2013, pp. 224-240.

[2] Qin Y., A review on the development of cool pavements to mitigate urban heat island effect, Renewable and Sustainable Energy Reviews, Vol. 52, 2015, pp. 445-459.

[3] Higashiyama H., Sano S., Nakanishi F., Takahashi O., and Tsukuma S., Field measurements of road surface temperature of several asphalt pavements with temperature rise reducing function, Case Studies in Construction Materials, Vol. 4, 2016, pp. 73-80.

[4] Higashiyama H., Sano S., Nakanishi F., Sugiyama M., Takahashi O. and Tsukuma S., Effect on surface temperature reduction of asphalt pavements with cement-based grouting materials containing ceramic waste powder, International Journal of Civil, Environment, Structural, Construction and Architecture Engineering, Vol. 10, No. 8, 2016, pp. 1014-1020.

[5] Zhou F., Scullion T. and Sun L., Verification and modeling of three-stage permanent deformation behavior of asphalt mixes, Journal of Transportation Engineering, ASCE, Vol. 130, No. 4, 2004, pp. 486-494.

[6] Xu Y. and Sun L., Study on permanent deformation of asphalt mixes by single penetration repeated shear test, Procedia-Social, and Behavioral Sciences, Vol. 96, 2013, pp. 886-893.

[7] Yinfei D., Jianqi C., Zheng H. and Weizheng L., A review on solutions for improving rutting resistance of asphalt pavement and test methods, Construction and Building Materials, Vol. 168, 2018, pp. 893-905.

[8] Higashiyama H. and Sano M., Fatigue resistance of surface temperature reducing pavement under fixed-point load, International Journal of GEOMATE, Vol. 13, Issue 35, 2017, pp. 166-173.

[9] Japan Road Association, Design Handbook for Pavements, 2006 (in Japanese).

[10] Japan Road Association, Japanese Specifications for Roadway Bridges, 2012 (in Japanese).

[11] Kubo K., Rational maintenance of the pavement of national highways, Construction Execution Project, No. 684, 2007, pp. 6-10 (in Japanese).

[12] Abe Y. and Iino T., A study on the numerical analysis of rutting depth data, Journal of Japan Society of Civil Engineers, No.478/V-21, 1993, pp. 117-123 (in Japanese).
[13] Japan Road Association, Pavement Performance Evaluation Method, 2008 (in Japanese).